Journal of Cardiovascular Nursing
Vol. 00, No. 0, pp. 00–00 | Copyright © 2021 Wolters Kluwer Health, Inc. All rights reserved.

# The Contribution of Thoracic Radiation Dose Volumes to Subsequent Development of Cardiovascular Disease in Cancer Survivors

Carolyn Miller Reilly, PhD, RN, CHFN-K, CNE, FAHA, FAAN; Melinda Higgins, PhD; Javed Butler, MD, MPH, FAHA; Natia Esiashvili, MD; Baowei Fei, PhD, EngD; Tommy Flynn, BSN; James D. Dormer, MS; Eduard Schreibmann, PhD, DABR



**Background:** Although radiation therapy (RT) has been recognized for contributing to cardiovascular disease (CVD), it is unknown whether specific doses received by cardiovascular tissues influence development. **Objective:** In this pilot study, we examined the contribution of RT dose distribution on the development of CVD events in patients with cancer within 5 years of RT. **Methods:** A retrospective case-controlled design was used matching 28 cases receiving thoracic RT who subsequently developed an adverse CVD event with 28 controls based upon age, gender, and cancer type. Dose volume histograms of nongated computed tomography scans received during RT characterized the dose delivered to the heart. Heart chambers were segmented using an atlas approach, and radiomics features for the segmentation as well as planning dose in each chamber were tabulated for analysis. **Result:** No significant differences were observed in the RT dose statistics between groups, preexisting CVD, nor significant differences of RT doses delivered to distinct chambers of the heart. Cases were found to have greater CVD risk factors at the time of cancer diagnosis. Morphological significant differences for perimeter on border ($P = .043$), equivalent spherical radius ($P = .050$), and elongation ($P = .038$) were observed, with preexisting CVD having the highest values (ie, larger hearts). **Conclusion:** Traditional CVD risk factors were more prevalent in the cases who developed CVD. No differences were observed in doses of RT. Of note, we observed significant differences in heart morphology and mass in known diseased hearts on the pretreatment scans. These new metrics may have implications for the measurement and quantification of CVD.

**KEY WORDS: cardiovascular disease, ionizing radiation, radiation-induced heart disease, radiobiology**

Since 1896, radiation has been used to cure cancer, and even today, more than 50% of patients with cancer receive radiation therapy (RT).[1] With RT, all vascular structures within the radiation field are vulnerable to injury due to endothelial dysfunction, progressive

**Carolyn Miller Reilly, PhD, RN, CHFN-K, CNE, FAHA, FAAN**
Professor, Clinical Nursing, Nell Hodgson Woodruff School of Nursing, Emory University, Atlanta, Georgia.

**Melinda Higgins, PhD**
Professor, Research and Senior Biostatistician, Nell Hodgson Woodruff School of Nursing, Emory University, Atlanta, Georgia.

**Javed Butler, MD, MPH, FAHA**
Professor, Patrick H. Lehan Chair in Cardiovascular Research, and Chairman of Department of Medicine, University of Mississippi Medical Center, Jackson, Mississippi.

**Natia Esiashvili, MD**
Professor and Chief Quality Officer, Department of Radiation Oncology, Winship Cancer Institute, Emory University, Atlanta, Georgia.

**Baowei Fei, PhD, EngD**
Professor and Cecil H. and Ida Green Chair in Systems Biology Science, Department of Bioengineering, Erik Jonsson School of Engineering and Computer Science, University of Texas at Dallas; and Department of Radiology, University of Texas Southwestern Medical Center, Dallas.

**Tommy Flynn, BSN**
PhD Candidate, Nell Hodgson Woodruff School of Nursing, Emory University, Atlanta, Georgia.

**James D. Dormer, MS**
Research Engineer, Scientist Associate II, Department of Bioengineeirng, Erik Jonsson School of Engineering and Computer Science, University of Texas at Dallas.

**Eduard Schreibmann, PhD, DABR**
Associate Professor, Department of Radiation Oncology, Winship Cancer Institute, Emory University, Atlanta, Georgia.

The project has been funded at least in part by the National Cancer Institute (NCI) via NCI Community Oncology Research Program, a member of the NCI National Clinical Trials Network with federal funds from the Department of Health and Human Services under grant number UG1CA189867. The contents of this publication do not necessarily reflect the views or policies of the Department of Health and Human Services, nor does it imply endorsement by the US Government.

The authors have no conflicts of interest to disclose.

**Correspondence:**
Carolyn Miller Reilly, PhD, RN, CHFN-K, CNE, FAHA, Nell Hodgson Woodruff School of Nursing, Emory University, 1520 Clifton Rd, #366 Atlanta, GA 30322 (carolyn.reilly@emory.edu).

DOI: 10.1097/JCN.0000000000000834

microvascular damage, initiation of fibrosis, and persistent inflammation.[2]

Risk of total cardiovascular disease (CVD) is increased in cancer survivors who received thoracic radiotherapy. Radiation therapy to the chest increases the risk of heart disease based upon the cumulative dose of radiation, with an estimated aggregate CVD incidence of 10% to 30% within 5 to 10 years of treatment.[3] Well recognized is a further increase in the risk of CVD when combined with cardiotoxic chemotherapeutic agents such as anthracyclines in a similar dose-dependent fashion.[4,5]

These CVD complications encompass a range of deleterious effects on the heart, from subclinical histopathological changes to overt clinical disease involving the pericardium, myocardium, valves, conduction system, and coronary arteries.[6] Within the pericardium, disruption of microvascular endothelial cells with repeated episodes of ischemia leads to fibrosis and eventual collagen deposits.[7] Myocardial damage results from continual fibrotic remodeling of the myocardium and destruction of myocardial capillaries by collagen deposition.[8] The cardiac valves experience RT-induced fibrotic thickening, calcification, and valve retraction. Radiation therapy–induced changes affect the conduction system from several fronts including altering the baroreceptor reflex and inducing autonomic dysfunction,[9,10] and diffuse fibrosis of the sinoatrial node and conduction pathways.[11] Finally, within the coronary vessels, endothelial dysfunction leads to persistent inflammation and progressive microvascular damage,[2] accelerating atherosclerosis, independent of other CVD risk factors.

Although RT has long been recognized for its contribution to CVD,[4,5] it is unknown whether doses of radiation received by specific cardiovascular tissues can account for the development of CVD. We set out to extract and analyze a comprehensive set of features from the radiation treatment plans including dose volume histograms (DVHs) developed from the 3-dimensional dose distribution, computed tomography (CT) image, and anatomical structures. These were collected and analyzed using in-house custom software, providing detailed radiation dose distribution and anatomical-spatial characteristics such as overlap of heart with the high-dose area. This allowed for the development of detailed 3-dimensional dose volume analyses using a heart atlas (left ventricle, right ventricle, left atrium, right atrium, pulmonary arteries/aorta/coronary arteries) in patients who received RT for intrathoracic malignancies.[12]

The purpose of this pilot study was to examine the contribution of RT dose distribution on the development of any significant CVD events (defined as pericarditis, myocardial infarction, coronary artery disease, valvular heart disease, heart rhythm disturbances, or heart failure requiring medical care) in 56 patients with cancer within 5 years of receiving RT to the thoracic region using a retrospective case-controlled design. We hypothesized that cases with an adverse CVD event would be associated with greater dose volume amounts of radiation, when controlling for typical CVD risk factors.

## Methods

### Design

A retrospective case-controlled design was used allowing for the medical records and images of 28 patients receiving thoracic radiation who subsequently developed an adverse CVD event to be matched with 28 controls based on age, gender, and cancer type.

### Sample

After obtaining institutional review board approval as an exempt study, all patients receiving therapeutic thoracic radiation for a cancer between 2003 and 2008

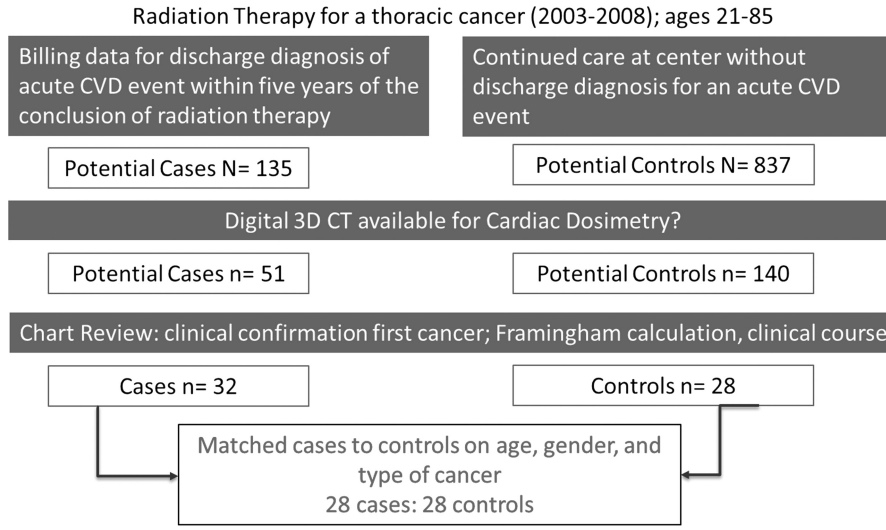


**FIGURE 1.** *Case and control selection and matching.*

and who subsequently received treatment for an adverse CVD event within 5 years of completing their RT (Figure 1) were identified as potential cases via billing records. Possible controls were identified through a similar second culling of persons receiving chest RT who met inclusion criteria but did not experience a subsequent adverse CVD event. Final selection as a case or control was based upon assurance of stored baseline digital 3-dimensional CT (3D CT)–based dose plans for dosimetry assessment. Medical record review was then undertaken for all clinical data and calculated CVD risk in both groups. Cases were matched to controls based upon age range, gender, and type of cancer.

Inclusion criteria for both cases and controls included age of 21 to 85 years and completion of chest RT within the preceding 10 years. In the CVD case group, patients experienced a readmission for an acute CVD event within 5 years of the conclusion of RT. Specific CVD events were isolated to those directly attributable to thoracic radiation and included pericarditis, myocardial infarction, coronary artery disease leading to myocardial compromise or requiring revascularization, valvular heart disease, heart rhythm disturbances, or heart failure. As provided in Table 1, we noted that most cases developed coronary artery disease requiring hospitalization and intervention, followed by heart failure, whereas only a small percentage developed valvular or rhythm disorders (primarily atrial fibrillation), and none experienced pericarditis.

Exclusion criteria for both cohorts included death attributed to cancer within the 5-year period. (Patients

**TABLE 1 Demographic, Clinical, Cardiovascular Risk, and Cancer Treatment Variables**

| | All N = 56 | Cases N = 28 | (A) Controls N = 28 | | (B) Cases (No CVD) N = 22 | (C) Cases (CVD History) N = 6 | |
|---|---|---|---|---|---|---|---|
| | Mean (SD) / Med [IQR] / n (%) | Mean (SD) / Med [IQR] / n (%) | Mean (SD) / Med [IQR] / n (%) | Test Cases/ Controls | Mean (SD) / Med [IQR] / n (%) | Mean (SD) / Med [IQR] / n (%) | Test A/B/C |
| Demographics | | | | | | | |
| Age, y | 62.1 (8.9) | 62.3 (8.9) | 61.9 (9.0) | .882[a] | 64.4 (7.5) | 54.5 (10.1) | .049[f] |
| Male | 17 (30.4%) | 8 (28.6%) | 9 (32.1%) | .771[c] | 5 (22.7%) | 3 (50.0%) | .448[g] |
| Cancer type | | | | | | | |
| Lung* | 16 (28.6%) | 9 (32.1%) | 7 (25.0%) | .584[c] | 6 (27.3%) | 3 (50.0%) | .389[g] |
| Breast | 34 (60.7%) | 16 (57.1%) | 18 (64.3%) | | 14 (63.6%) | 2 (33.3%) | |
| Thyroid* | 1 (1.8%) | 1 (3.6%) | 0 (0%) | | 1 (4.5%) | 0 (0%) | |
| Metastatic* | 2 (3.6%) | 1 (3.6%) | 1 (3.6%) | | 0 (0%) | 1 (16.7%) | |
| Other* | 3 (5.4%) | 1 (3.6%) | 2 (7.1%) | | 1 (4.5%) | 0 (0%) | |
| African American | 22 (39.3%) | 13 (46.4%) | 9 (32.1%) | .274[c] | 10 (45.5%) | 3 (50.0%) | .537[g] |
| CVD risk variables at cancer diagnosis | | | | | | | |
| BMI | 29.6 (7.2) | 31.8 (7.9) | 27.3 (5.7) | .019[b] | 32.5 (8.0) | 29.4 (7.8) | .040[f] |
| Systolic BP | 132.0 (17.1) | 137.1 (16.4) | 126.9 (16.5) | .025[a] | 141.8 (11.5) | 119.7 (20.9) | .001[f] |
| Glucose level | *108 [98, 124]* | *113 [97, 173]* | *105 [98, 114]* | .089[d] | *109.5 [99, 154]* | *136.5 [91.5, 234.3]* | .209[e] |
| Framingham risk | 19.9 (10.1) | 23.4 (9.2) | 16.3 (9.9) | .008 [a] | 24.0 (7.8) | 21.0 (13.9) | .033[h] |
| Family history CVD | 20 (36.4%) | 13 (48.1%) | 7 (25.0%) | .074[c] | 10 (47.6%) | 3 (50.0%) | .202[g] |
| History of hypertension | 38 (67.9%) | 22 (78.6%) | 16 (57.1%) | .086[c] | 18 (81.8%) | 4 (66.7%) | .166[g] |
| Smoker history | 13 (23.2%) | 9 (32.1%) | 4 (14.3%) | .114[c] | 5 (22.7%) | 4 (66.7%) | .025[g] |
| Diabetes history | 15 (26.8%) | 13 (45.4%) | 2 (7.1%) | .001[c] | 8 (36.4%) | 5 (83.3%) | <.001[g] |
| Cancer variables | | | | | | | |
| Chemotherapy | 32 (57.1%) | 19 (67.9%) | 13 (46.4%) | .105[c] | 15 (68.2%) | 4 (66.7%) | .290[g] |
| Hormone therapy (N = 46) | 17 (37.8%) | 5 (27.8%) | 12 (44.4%) | .259[c] | 3 (23.1%) | 2 (40.0%) | .437[g] |
| Radiation duration (n = 53) | *42 [35, 45.8]* | *42 [23.5, 45.5]* | *42 [35, 46]* | .640[d] | *50 [30, 45]* | *44.5 [13, 51.9]* | .752[e] |
| Cancer stage | *2 [1, 3]* | *3 [1.3, 3.8]* | *1 [1, 2.8]* | .002[d] | *3 [1, 3.3]* | *3 [2.5, 4.0]* | .008[e] |
| 0 | 3 (5.4%) | 0 (0%) | 3 (10.7%) | | 0 (0%) | 0 (0%) | |
| 1 | 19 (33.9%) | 7 (25.0%) | 12 (42.9%) | | 6 (27.3%) | 1 (16.7%) | |
| 2 | 8 (14.3%) | 2 (7.1%) | 6 (21.4%) | | 2 (9.1%) | 0 (0%) | |
| 3 | 17 (30.4%) | 12 (42.9%) | 5 (17.9%) | | 9 (40.9%) | 3 (50.0%) | |
| 4 | 9 (16.1%) | 7 (25.0%) | 2 (7.1%) | | 5 (22.7%) | 2 (33.3%) | |
| Primary endpoints (some patients developed more than 1 disease state) | | | | | | | |
| Coronary artery disease | | 17 (53%) | | | | | |
| Valvular disease | | 3 (9%) | | | | | |
| Rhythm disturbances | | 2 (6%) | | | | | |
| Heart failure | | 10 (31%) | | | | | |

* indicates categories combined for $\chi^2$ tests. [a] *t* Test pooled variance. [b] *t* Test unpooled variance. [c] $\chi^2$ Test. [d] Mann-Whitney test. [e] Kruskal-Wallis test. [f] Analysis of variance. [g] Fisher-Freeman-Halton exact test for R × C contingency tables. [h] Analysis of variance: Welch test.

who died secondary to the CVD event in question were included in this analysis.)

### Sample Size

We were able to identify 28 case-control matches for a final sample size of 56. With this sample size, we determined that we could detect moderate-to-large effect sizes at 80% power and 5% level of significance: effect sizes of $r = 0.50$ for correlation, $d = 0.76$ for $t$ test, $w = 0.37$ for a $\chi^2$ test for the difference of proportions between the 2 groups, and $r^2 = 0.36$ for a regression model with 3 tested predictors adjusting for up to 3 covariates.

## Variables and Measures

Data to measure study variables were abstracted from the electronic medical record and digitally stored images acquired during the RT.

- Demographic and clinical variables included age, gender, ethnicity, family history, total cholesterol, high-density lipoprotein cholesterol, smoking history, systolic blood pressure, body mass index, hypertension history, type of cancer, agents used and dosage, and total RT dosage.
- These baseline data were used to compute the Framingham Risk Score, a well-validated 10-year risk prediction instrument for general CVD.[13]
- Dependent CVD outcomes in cases were identified from the electronic medical record and included clinical diagnosis of pericarditis, myocardial infarction, coronary artery disease, valvular heart disease, heart rhythm disturbances, or heart failure.
- Table 2 provides definitions and references for radio-oncology variables used in this article.
  a. For an in-depth analysis of cardiac toxicity, we used atlas segmentation to automatically identify heart regions of clinical interest.[14–16] The atlas segmentation used expert labels identified by a radiation oncologist on a high-resolution scan as input to an automated and consistent segmentation procedure in radiotherapy. The approach relies on the existence of a mapping between a reference image volume (called atlas) in which structures of interest have been segmented and validated by an expert and the image to be segmented, called subject. A point-to-point mapping obtained by a deformable image registration is used to match the atlas with the image to be segmented. Once the point-wise transformation between the images was obtained, the same transformation was applied on the structures defined on the atlas data set to warp them onto the data set to be segmented. The

**TABLE 2 Definitions and References for Radio-oncology Terminology**

| Term | Definition |
|---|---|
| Dice coefficient | A general coefficient describing the overlap between 2 shapes. In this article, it describes the overlap between dose and a patient's organ. This normalized value is independent of the absolute volume and thus normalized across patients with a value of zero when the critical organ is outside the isodose in question and a value of 1 for a full overlap.[21,22] |
| Dose volume histograms | A type of graph commonly used in radiotherapy to represent the total dose of radiation delivered inside a patient organ. It is a cumulative histogram of the dose received in each voxel within the organ.[12] |
| Elongation 1–3 | Similar to the one mentioned previously, measures to describe a geometrical shape as the ratio of the largest to the smallest PCA coefficients. These measures are independent of an object's orientation in space.[12] |
| Equivalent spherical radius | The radius of a sphere having the same volume as an organ's geometrical representation.[12] |
| Gray | Gray is the standard unit to describe radiation doses in radiotherapy. It is defined as the absorption of 1 joule of radiation energy per kilogram of matter.[24] |
| Gray-level run length statistical features | Features describing an image's texture. Gray-level run length statistical features are extracted from a gray-level run length matrix, which is generated by counting the intensities in neighborhood pixels.[23] |
| Isodose levels | Similar to iso-levels on maps, these lines show regions of equal dose in radiotherapy treatment plans. These lines are displayed on top of images of the patient's anatomy, as a way to graphically show where the dose is deposited in a patient. |
| PCA0, PCA1, and PCA2 | Measures to describe a shape's appearance based on principal component analysis. An organ's geometrical representation is first interpreted to determine the principal components of variations. PCA0 to PCA2 represent the coefficients of such an analysis, describing variations along a shape's principal axes.[12] |
| Perimeter on border | Perimeter of an organ's geometrical representation.[12] |
| Perimeter, elongation, and flatness | Measures describing how flat or elongated a shape is based on PCA (described previously).[12] |
| Pixels on border | Number of pixels on the border of an organ's geometrical representation.[12] |
| Radiomics | Radiomics is an analytic approach that first extracts large amounts of quantitative features from radiologic images using data characterization algorithms followed by statistical analysis of features versus outcomes to identify predictive measures of outcomes.[23] |
| Roundness | A coefficient describing how "round" an organ segmentation is.[12] |
| Voxel | Used in 3-dimensional computer graphics, a voxel represents a value on a regular grid in 3-dimensional space. Comparable with pixels on a 2-dimensional bitmap, voxels themselves do not occupy a specific coordinate, but their position is inferred based upon its position relative to other voxels.[25] |
| Wavelet features | Wavelet features are first-order statistics after performing wavelet decomposition on the original image using high-pass and low-pass filters.[23] |

Abbreviation: PCA, principal component analysis.

algorithm output a set of labels that are superimposed on the data set to be segmented. As an automated clinically validated process,[17,18] the procedure not only significantly reduces clinician time to segment structures of interest[19] but also eliminates interobserver variability as the same template is used for all patient segmentations.[20]

b. To investigate whether treatment plan features were associated with adverse outcomes, we used in-house software to generate a set of measures characterizing the dose deposited and its spatial relationship to each region at risk as identified through the detailed heart atlas. Dose volume histograms for each heart compartment were tabulated in 1-gray (Gy) increments (from 1 to 30 Gy) on the x-axis, with the percentage of dose received (in absolute volume) by the critical organ receiving that dose level plotted along the y-axis. Because a DVH is a cumulative histogram of how many voxels inside an organ receive a given dose value, as the dose level increases, fewer voxels receive that higher amount of radiation and the graph diminishes toward zero. The last value is the maximum dose that is received by only a point (voxel) in the heart.
c. The volume of each compartment in the high-dose area was computed by the Dice coefficient between increments of isodose levels and a critical organ segmentation. Dice is a general geometrical measure that characterizes the degree of overlap between 2 blobs, which is independent of the absolute volume and thus normalized across patients with an assigned value of zero when the critical organ is outside the isodose in question and assigned a value of 1 for a full overlap.[21,22]
d. Measures of dose inhomogeneity used concepts derived from image analysis to detail the local deposition of dose beyond the mean values used in clinical practice. The dose deviation from the mean through the standard deviation, maximum value, and measures of dose inhomogeneity for each voxel in the heart were recorded.

All data were de-identified, entered into a database, and maintained on a password-protected secure computer. Data were reviewed for completeness and data entry errors, and variables were reviewed for assumptions of normality. Nonparametric statistical tests were used for variables that were skewed and did not meet normality assumptions. Correlations (for 2 continuous measures), *t* tests, and/or analysis of variance (ANOVA) (1 continuous, 1 categorical with 2 or more categories) or the nonparametric equivalents (Mann-Whitney or Kruskal-Wallis tests) and $\chi^2$ tests were used. Multivariate ANOVA (MANOVA) was performed for measures that made logical sense to assess together with 3-dimensional shape metrics, such as principal component analysis (PCA) 0, 1, and 2 and elongation 1, 2, and 3; post hoc ANOVAs were further performed for each measure individually under the family-wise error rate for the overall MANOVA model. However, other pairwise error rate corrections for multiple statistical tests were not performed because the goal of these analyses was primarily meant to be descriptive and provide estimates from a pilot study in an area where little statistics have been previously reported. Logistic regression was used with the likelihood ratio variable selection method to create the most parsimonious model describing the relationships of DVHs, radiation dose metrics, cardiovascular risk factors, and demographics for the development of adverse CVD events. While patients were matched based upon age range, gender, and type of cancer, an examination of other possible covariates such as body mass index was evaluated and adjusted for in the final statistical model. Variables were considered for inclusion in the final model if the univariate tests had $P \leq .10$. These variables considered were as follows: age, body mass index, glucose level, Framingham Risk Score hypertension history, smoking history, chemotherapy, cancer stage, systolic blood pressure and radiation metrics (pixels on border, perimeter on border, equivalent spherical radius, roundness, perimeter, elongation, flatness, PCA0, PCA1, PCA2, elongation1, elongation2, elongation3) (Table 2). All statistical analyses were performed with SPSS v.23 at the 5% significance level.

## Results

All case-to-control matching was appropriate for age at cancer diagnosis (cases, 62.3 ± 8.9; controls, 61.9 ± 9.0; $P = .882$), gender ($P = .771$), and most cancer types ($P = .584$). For cancer type, all 16 breast cases matched to 16 breast controls, 9 lung cases matched to 7 lung controls and 2 metastasis controls, 1 metastatic case matched to a metastatic control, and 1 thyroid and 1 other case matched to 2 other controls (Table 1).

### Traditional Cardiovascular Disease Risk Differences Pre Cancer Treatment

Significant differences in most CVD risk factors were observed between cases and controls at the diagnosis of cancer, as summarized in Table 1. Specifically, patients who developed CVD had multiple typical risk factors at the time of their cancer diagnosis, whereas the controls did not, including significantly higher body mass index ($P = .02$), significantly higher systolic blood pressure ($P = .03$), and significantly higher Framingham Risk Score ($P = .01$) and rates of diabetes ($P = .01$). Although the cases had a significantly later stage of cancer ($P = .01$) and there may have been variability in the exact type of chemotherapy agents, there were no differences between cases and controls in receipt of chemotherapy or hormone agents.

Importantly, 6 of the 28 cases (21.4%) had a history of preexisting CVD (ie, previous myocardial infarction, history of heart failure, or treatment of coronary artery disease with an interventional procedure) compared with none of the 28 controls. Given this difference, we also ran comparisons between the controls, cases without preexisting CVD, and cases with preexisting CVD. Cases with preexisting CVD were significantly younger at the time of the study by 10 years ($P = .02$), were more likely to smoke (4/6, 66.7%, $P = .03$), and have diabetes (5/6, 83.3%, $P < .001$). It is also noted that 83.3% (5/6) of the cases

with preexisting CVD had a cancer stage of 3 or 4 compared with 63.6% of the cases without preexisting CVD and only 25% of the controls ($P$ = .01) (Table 1). The cardiovascular outcome precipitating inclusion as a CVD case was ischemic coronary artery disease for 4 of the patients and heart failure with reduced ejection fraction secondary to hypertension for the other 2 patients. Notably, the average time from radiation treatment to the subsequent CVD event averaged 41.33 months for these 6 patients, whereas the other 22 cases experienced an event much earlier at an average of 29 months.

## Dose Volume Statistics

There were no significant differences between the radiation doses for the cases and controls, for cases with and without preexisting CVD versus controls, nor significant differences between the radiation doses delivered to distinct chambers of the heart. Furthermore, although the percent average DVH levels were higher for the cases than the controls (Figure 2), none was statistically significantly different. This is most pronounced at DVH 06 to 08, as seen in Figure 2. Although not statistically significant, the DVH values of 1 to 30 Gy are all consistently higher for the cases without preexisting CVD than for the controls, but the 6 cases with preexisting CVD had the lowest values, as evidenced by Figure 2, potentially because of larger heart profiles observed in cases with preexisting CVD.

## Cardiac Silhouette Pretreatment Differences

Using traditional measures and visualization, there were no significant differences between cardiac shape measures between the matched case-control pairs on most of the pretreatment scans. Using MANOVA for PCA0, PCA1, and PCA2, there were no significant differences between cases and controls ($P$ = .20), nor when considering elongation1, elongation2, and elongation3 ($P$ = .21). However, cases with a known history of CVD were observed to have greater PCA2 and elongation3 ($P$ < .15) that approached significance (Table 3), stimulating further statistical and computational exploration.

To ascertain whether this morphological difference was due to possible structural changes from preexisting CVD, we then evaluated these cases individually compared with those cases without preexisting CVD, observing significant differences for perimeter on border ($P$ = .04), equivalent spherical radius ($P$ = .05), and elongation ($P$ = .04), with the cases with preexisting CVD having the highest values (ie, larger hearts). Using MANOVA for PCA0, PCA1, and PCA2, there was a borderline significant difference between controls, and cases with and without preexisting CVD ($P$ = .07), with significant post hoc ANOVA differences specifically for PCA0 ($P$ = .04) and PCA2 ($P$ = .05). Similarly, borderline significant differences were seen between controls and cases with and without preexisting CVD when considering elongation1, elongation2, and elongation3 ($P$ = .08), with specific significant post hoc ANOVA differences for elongation1 ($P$ = .04) and elongation3 ($P$ = .04). In both the PCA0 to PCA2 and elongation1 to elongation3 measures, the cases with preexisting CVD had the largest dimensional measurements.

## Radiomics

Given these baseline differences between specific aspects of the cardiac silhouette, we sought further analysis and confirmation of these differences using radiomics. Radiomics is an analytic approach that extracts large amounts of quantitative features from radiologic images using data characterization algorithms. In this work, we focus on 2 groups of radiomic features: first-order wavelet features and gray level run length (GLRL) statistical features.[23] Wavelet features are first-order statistics after performing wavelet decomposition on the original image using high-pass and low-pass filters. Gray-level run-length statistical features are extracted from a GLRL matrix, which is generated by counting the number of consecutive identical pixels. We compared the difference

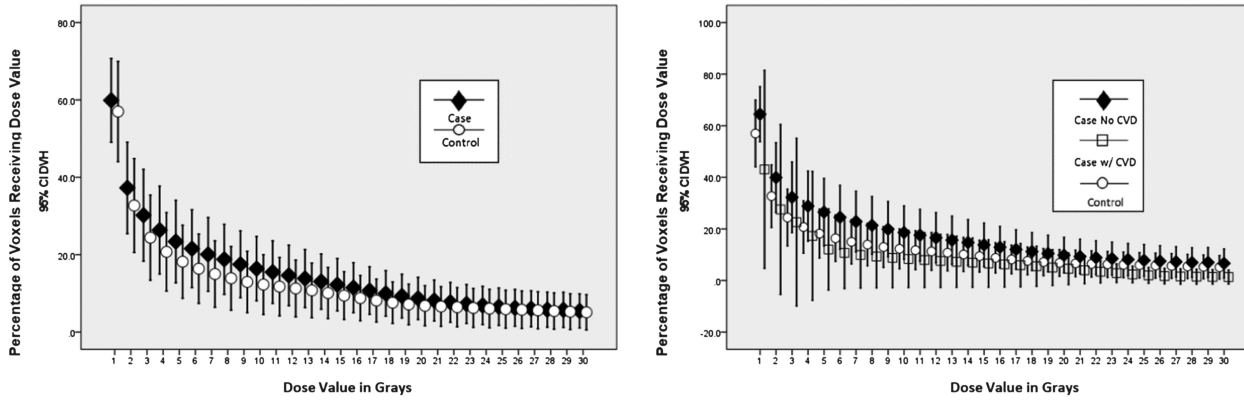


**FIGURE 2.** *Dose volume histograms.*

**TABLE 3 Radiation Shape Metrics Between All Cases With and Without Preexisting Cardiovascular Disease and Controls**

| | | | | | | Percentiles | | | ANOVA |
|---|---|---|---|---|---|---|---|---|---|
| | | Mean | SD | Min | Max | 25th | Median | 75th | *P* |
| Pixels on border | 0 control | 1.32 | 0.11 | 1.06 | 1.60 | 1.27 | 1.30 | 1.36 | .557 |
| | 1 case - no CVD | 1.35 | 0.11 | 1.17 | 1.58 | 1.27 | 1.35 | 1.42 | |
| | 2 case - CVD | 1.37 | 0.11 | 1.22 | 1.50 | 1.27 | 1.38 | 1.46 | |
| Perimeter on border | 0 control | 33 772.24 | 5239.20 | 19 912.30 | 43 072.20 | 30 025.13 | 33 735.15 | 37 557.70 | .043 |
| | 1 case - no CVD | 33 491.79 | 6878.34 | 22 788.20 | 51 266.70 | 28 319.98 | 33 896.15 | 35 740.58 | |
| | 2 case - CVD | 40 422.82 | 6683.42 | 32 389.80 | 52 065.80 | 35 709.98 | 39 516.20 | 44 690.60 | |
| Equivalent spherical radius | 0 control | 51.68 | 4.14 | 39.81 | 58.55 | 48.88 | 51.81 | 54.67 | .050 |
| | 1 case - no CVD | 51.38 | 5.20 | 42.58 | 63.87 | 47.47 | 51.94 | 53.33 | |
| | 2 case - CVD | 56.56 | 4.60 | 50.77 | 64.37 | 53.29 | 56.06 | 59.57 | |
| Roundness | 0 control | 1.37 | 0.16 | 1.16 | 1.85 | 1.26 | 1.36 | 1.44 | .344 |
| | 1 case - no CVD | 1.43 | 0.15 | 1.15 | 1.75 | 1.31 | 1.42 | 1.54 | |
| | 2 case - CVD | 1.34 | 0.13 | 1.18 | 1.54 | 1.23 | 1.33 | 1.44 | |
| Perimeter | 0 control | 46 744.15 | 7822.08 | 23 629.40 | 61 113.20 | 43 774.08 | 47 050.00 | 52 036.03 | .287 |
| | 1 case - no CVD | 48 519.22 | 13 528.27 | 30 866.20 | 89 732.70 | 39 200.48 | 46 204.00 | 53 252.75 | |
| | 2 case - CVD | 54 288.42 | 8755.27 | 40 586.20 | 66 868.90 | 47 790.25 | 55 010.30 | 60 264.63 | |
| Elongation | 0 control | 588 760.36 | 133 254.80 | 264 214.00 | 840 561.00 | 489 254.00 | 582 637.00 | 684 431.25 | .038 |
| | 1 case - no CVD | 584 897.00 | 183 597.80 | 323 474.00 | 1 091 510.00 | 448 138.50 | 586 823.50 | 635 430.75 | |
| | 2 case - CVD | 770 643.00 | 194 485.46 | 548 134.00 | 1 117 130.00 | 635 231.50 | 739 118.50 | 891 352.25 | |
| Flatness | 0 control | 0.73 | 0.08 | 0.59 | 0.86 | 0.67 | 0.73 | 0.78 | .253 |
| | 1 case - no CVD | 0.70 | 0.06 | 0.57 | 0.83 | 0.66 | 0.71 | 0.74 | |
| | 2 case - CVD | 0.75 | 0.06 | 0.65 | 0.80 | 0.69 | 0.77 | 0.79 | |
| MANOVA (PCA0, PCA1, PCA2); $F_{6,104} = 1.990$, $P = .074$ | | | | | | | | | |
| PCA0 | 0 control | 310.05 | 70.97 | 169.49 | 447.10 | 258.22 | 308.76 | 360.15 | .039 |
| | 1 case - no CVD | 285.08 | 65.75 | 165.31 | 444.18 | 249.89 | 270.38 | 315.08 | |
| | 2 case - CVD | 368.66 | 77.96 | 284.38 | 487.03 | 296.23 | 359.89 | 437.19 | |
| PCA1 | 0 control | 573.20 | 112.75 | 302.40 | 866.36 | 494.52 | 586.76 | 636.02 | .310 |
| | 1 case - no CVD | 572.24 | 127.90 | 361.62 | 836.92 | 485.26 | 552.68 | 652.62 | |
| | 2 case - CVD | 653.48 | 130.49 | 510.83 | 844.36 | 563.28 | 600.31 | 799.34 | |
| PCA2 | 0 control | 990.44 | 154.55 | 603.88 | 1410.72 | 878.55 | 992.43 | 1073.47 | .048 |
| | 1 case - no CVD | 1038.41 | 238.70 | 610.66 | 1700.69 | 842.02 | 1025.76 | 1135.22 | |
| | 2 case - CVD | 1215.42 | 212.03 | 952.68 | 1520.13 | 1014.24 | 1202.53 | 1414.97 | |
| MANOVA (Elongation1, Elongation2, Elongation3); $F_{6,104} = 1.969$, $P = .077$ | | | | | | | | | |
| Elongation1 | 0 control | 76.90 | 9.07 | 57.03 | 93.46 | 70.42 | 77.39 | 83.28 | .041 |
| | 1 case - no CVD | 73.84 | 8.45 | 56.31 | 91.98 | 69.47 | 72.55 | 78.37 | |
| | 2 case - CVD | 84.34 | 8.88 | 74.26 | 97.16 | 75.86 | 83.70 | 92.39 | |
| Elongation2 | 0 control | 104.70 | 10.50 | 76.58 | 128.48 | 97.43 | 106.49 | 111.33 | .281 |
| | 1 case - no CVD | 104.64 | 11.64 | 83.43 | 127.56 | 96.96 | 103.49 | 112.57 | |
| | 2 case - CVD | 112.34 | 11.03 | 99.52 | 127.93 | 104.91 | 108.07 | 124.80 | |
| Elongation3 | 0 control | 137.89 | 10.80 | 108.22 | 163.65 | 130.81 | 138.61 | 144.55 | .042 |
| | 1 case - no CVD | 140.93 | 15.85 | 108.42 | 179.99 | 127.24 | 140.13 | 148.06 | |
| | 2 case - CVD | 153.33 | 13.21 | 136.67 | 171.65 | 140.40 | 153.04 | 165.86 | |

Abbreviations: ANOVA = analysis of variance; CVD = cardiovascular disease; MANOVA = multivariate analysis of variance; Max = maximum; Min = minimum.

between the control patients, cases with preexisting CVD, and cases without CVD. In addition, cases with and without preexisting CVD were compared with each other. As shown in Figure 3, the wavelet and GLRL features were significantly different between the controls, cases with preexisting CVD, and cases without preexisting CVD. Further analysis on a large patient population will help determine the clinical value of these features in possibly identifying patients with preexisting CVD and those at risk for developing such.

## Risk Modeling

Originally, we hypothesized that cases with an adverse CVD event would have received greater dose volume amounts of radiation and not have a greater number of CVD risk factors; only the opposite was observed. The cases all had significantly greater typical CVD risk factors upon cancer diagnoses and did not receive any greater or differing amounts of thoracic radiation. A logistic regression model (Table 4) was developed using the identified risk factors for the development of CVD with forward variable selection likelihood ratio methods used to choose the best set of variables. When modeling the cases (both with and without preexisting CVD) versus the controls, the resulting model retained cancer stage and body mass index, with no other demographic and clinical risk factors or radiation parameters (dose, DVH, or shape) entering the model. The coefficients

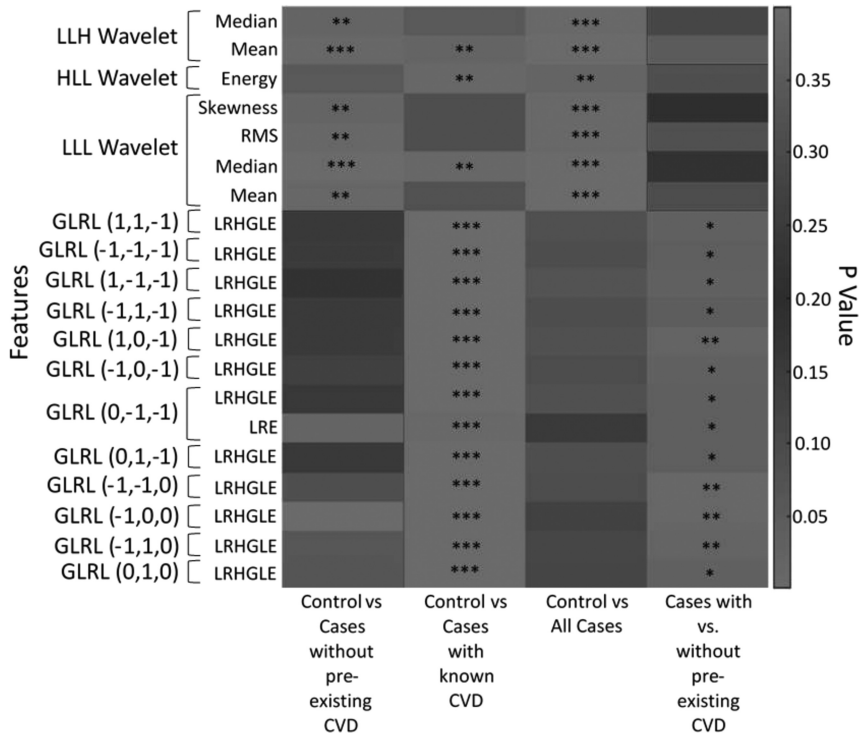


**FIGURE 3.** *Case and Control Selection and Matching.*

**TABLE 4 Logistic Regression Models for Cardiovascular Disease Events After Cancer Treatment**

**Cases vs Controls (n = 55, 1 Subject Missing Glucose)**

| | | | | | | | | 95% CI for OR | |
|---|---|---|---|---|---|---|---|---|---|
| | | *B* | $SE_B$ | Wald | *df* | *P* | OR | Lower | Upper |
| Step 1[a] | Cancer stage | 0.737 | 0.260 | 8.017 | 1 | .005 | 2.089 | 1.255 | 3.479 |
| | Constant | −1.578 | 0.640 | 6.077 | 1 | .014 | 0.206 | | |
| Step 2[b] | BMI | 0.120 | 0.049 | 5.952 | 1 | .015 | 1.128 | 1.024 | 1.242 |
| | Cancer stage | 0.834 | 0.283 | 8.655 | 1 | .003 | 2.302 | 1.321 | 4.013 |
| | Constant | −5.322 | 1.737 | 9.381 | 1 | .002 | 0.005 | | |

[a] Variable(s) entered on step 1: cancer stage
[b] Variable(s) entered on step 2: BMI
Final model: $\chi^2(df = 2) = 16.581$, $P < .001$
−2LL = 59.647, Nagelkerke $R^2 = 0.347$
72.7% overall correct classification

**Controls vs Cases Without CVD (n = 49, 6 Cases With CVD Removed)**

| | | | | | | | | 95% CI for OR | |
|---|---|---|---|---|---|---|---|---|---|
| | | *B* | $SE_B$ | Wald | *df* | *P* | OR | Lower | Upper |
| Step 1[a] | SBP (in 10-point units) | 0.839 | 0.284 | 8.767 | 1 | .003 | 2.315 | 1.328 | 4.036 |
| | Constant | −11.484 | 3.847 | 8.911 | 1 | .003 | 0.000 | | |
| Step 2[b] | Cancer stage | 0.685 | 0.291 | 5.562 | 1 | .018 | 1.984 | 1.123 | 3.507 |
| | SBP (in 10-point units) | 0.916 | 0.328 | 7.791 | 1 | .005 | 2.500 | 1.314 | 4.759 |
| | Constant | −13.986 | 4.620 | 9.165 | 1 | .002 | 0.000 | | |
| Step 3[c] | BMI | 0.113 | 0.061 | 3.423 | 1 | .064 | 1.120 | 0.993 | 1.263 |
| | Cancer stage | 0.791 | 0.323 | 6.001 | 1 | .014 | 2.206 | 1.171 | 4.154 |
| | SBP (in 10-point units) | 0.826 | 0.328 | 6.355 | 1 | .012 | 2.284 | 1.202 | 4.341 |
| | Constant | −16.431 | 5.082 | 10.454 | 1 | .001 | 0.000 | | |

[a] Variable(s) entered on step 1: systolic blood pressure (in 10-point units)
[b] Variable(s) entered on step 2: cancer stage
[c] Variable(s) entered on step 3: BMI
Final model: $\chi^2(df = 3) = 23.695$, $P < .001$
−2LL = 43.723, Nagelkerke $R^2 = 0.513$
77.6% overall correct classification

Abbreviations: BMI = body mass index; CI = confidence interval; CVD = cardiovascular disease; *df* = degrees of freedom; OR = odds ratio; SBP = systolic blood pressure; SE = standard error.

### What's New and Important?

- We observed that the development of CVD in the 5 years after cancer treatment was not associated with the RT dose distribution.
- Traditional CVD risk factors of elevated body mass index and elevated systolic blood pressure, along with advanced cancer stage, were correlated with the development of CVD within 5 years of RT.
- Differences in heart morphology and mass between known diseased hearts and those without disease were observed on baseline CT scans. No previous work has quantified reference values for these measures, and this small pilot may serve to stimulate further research into the clinical and research implications of such a measurement.

revealed that, for every 1-point increase in body mass index, the odds of developing CVD after cancer treatment was 1.13 times higher and every increase in cancer stage increased by 2.3 times the odds of developing CVD (Table 4, top). An additional model was run removing the 6 cases with preexisting CVD, and this model similarly retained body mass index, cancer stage, and systolic blood pressure (Table 4, bottom).

## Discussion

Our findings were quite intriguing, negating our hypothesis that the early development of CVD in the 5 years after cancer treatment would be associated with the RT dose distribution. In fact, no relationship between RT dose as calculated by DVH to areas of the heart was observed. Previously identified risk factors for CVD were associated with the development of CVD in our patients with cancer, with specific factors contributing the greatest risk including elevated body mass index and elevated systolic blood pressure. Interestingly, we observed that the greater stage of cancer at diagnosis, perhaps reflecting later time of diagnosis, was also associated with subsequent development of CVD after treatment.

One of the more confounding elements of this analysis was the observation that persons with preexisting CVD had morphological differences in their hearts on the baseline CT. These measures have not been previously described in detail, and no norms for these measures have been previously published. We propose that the mean values listed in Table 3 may serve as reference norms for persons at risk for the development of CVD, those without risk, and those with known CVD. Clearly, this requires subsequent study and evaluation because this was a post hoc finding of this small pilot study, undertaken only to explain the variability we observed.

This finding may hold clinical relevance in that we observed the DVHs of doses of radiation delivered to those with preexisting CVD were smaller. This may reflect not taking into consideration the greater mass and dimensions of a diseased heart when calculating the maximal safe dosage that should be delivered. On the basis of the preliminary results of the radiomics analysis, some features may be used to identify patients at risk for CVD before and after RT. A study with more comprehensive analyses of a large patient population is warranted in our future research.

### *Limitations*

Limitations of this retrospective chart review include the following:

1. The dose deposition in this study was computed using a standard 3D CT data set, in accordance to current clinical practice. However, these data sets do not capture cardiac and thoracic motion that may interfere with the dose delivery. Further metrics such as the distance between each chamber and beam should be explored in the future.
2. Because the goal of these analyses was primarily meant to be descriptive and provide estimates from a pilot study in an area where little quantification has been previously reported, no pairwise error rate corrections for multiple statistical tests were performed. The feature analysis is based on a limited number of patients, and a large study will help determine the clinical value of the measurements for identifying patients at risk.
3. A third limitation for this pilot is the fact that storing of baseline digital 3D-CT–based dose plans from which the computed radiologic and radiomic metrics were derived is a relatively new process. No files were available before 2003, limiting the number of patients who could have been accessed. As radiation-induced cardiovascular complications are a relatively later complication, we were unable to identify CVD events past 5 years and closer to the expected 10 years described in the literature. Thus, the CVD events described may not be a result of or hastened by RT.
4. Finally, retrospective studies are hindered by incomplete medical records, such as missing (or unmeasured) cholesterol levels, weights, and inability to capture CVD events that may have occurred but were treated at another facility.

## Conclusions

We found that the biggest difference between the cases of patients who developed CVD versus the controls who did not were traditional CVD risk factors at cancer diagnosis. No differences were observed in the radiation treatment. Of note, however, were differences found on the pretreatment imaging scans, which suggest differences in heart morphology and mass between known diseased hearts and those without disease. No previous work has quantified reference values for these measures, and this small pilot may serve to stimulate further research into the clinical and research implications of such a measurement.

Certainly, these findings support that a comprehensive assessment for traditional CVD risk factors combined with cardiac risk counseling may be warranted

for persons with thoracic cancers. It also suggests that baseline CT measurement of the heart and assessment of DVH of radiation delivered may be useful in maximizing the safe delivered dosage.

## REFERENCES


1. Baskar R, Lee KA, Yeo R, Yeoh K-W. Cancer and radiation therapy: current advances and future directions. *Int J Med Sci*. 2012;9(3):193–199. doi:10.7150/ijms.3635.
2. Totzeck M, Schuler M, Stuschke M, Heusch G, Rassaf T. Cardio-oncology—strategies for management of cancer-therapy related cardiovascular disease. *Int J Cardiol*. 2019;280:163–175. https://doi.org/10.1016/j.ijcard.2019.01.038.
3. Carver JR, Shapiro CL, Ng A, et al. American Society of Clinical Oncology clinical evidence review on the ongoing care of adult cancer survivors: cardiac and pulmonary late effects. *J Clin Oncol Off J Am Soc Clin Oncol*. 2007;25(25):3991–4008. doi:10.1200/jco.2007.10.9777.
4. Meyer RM, Gospodarowicz MK, Connors JM, et al. ABVD alone versus radiation-based therapy in limited-stage Hodgkin's lymphoma. *N Engl J Med*. 2012;366(5):399–408. doi:10.1056/NEJMoa1111961.
5. Shapiro CL, Hardenbergh PH, Gelman R, et al. Cardiac effects of adjuvant doxorubicin and radiation therapy in breast cancer patients. *J Clin Oncol*. 1998;16(11):3493–3501.
6. Heidenreich PA, Kapoor JR. Radiation induced heart disease: systemic disorders in heart disease. *Heart*. 2009;95(3):252–258. doi:10.1136/hrt.2008.149088.
7. Fajardo LF. The unique physiology of endothelial cells and its implications in radiobiology. *Front Radiat Ther Oncol*. 1989;23:96–112. doi:10.1159/000416574.
8. Liu LK, Ouyang W, Zhao X, et al. Pathogenesis and prevention of radiation-induced myocardial fibrosis. *Asian Pac J Cancer Prev*. 2017;18(3):583–587. doi:10.22034/apjcp.2017.18.3.583.
9. Groarke JD, Tanguturi VK, Hainer J, et al. Abnormal exercise response in long-term survivors of Hodgkin lymphoma treated with thoracic irradiation: evidence of cardiac autonomic dysfunction and impact on outcomes. *J Am Coll Cardiol*. 2015;65(6):573–583. doi:10.1016/j.jacc.2014.11.035.
10. Schultz-Hector S, Trott KR. Radiation-induced cardiovascular diseases: is the epidemiologic evidence compatible with the radiobiologic data? *Int J Radiat Oncol Biol Phys*. 2007;67(1):10–18. doi:10.1016/j.ijrobp.2006.08.071.
11. Slama MS, Le Guludec D, Sebag C, et al. Complete atrioventricular block following mediastinal irradiation: a report of six cases. *Pacing Clin Electrophysiol*. 1991;14(7):1112–1118. doi:10.1111/j.1540-8159.1991.tb02842.x.
12. Padfield D, Miller J. A Label Geometry Image Filter for Multiple Object Measurement. The Insight Journal. 2008. http://hdl.handle.net/1926/1493http://hdl.handle.net/1926/1493.
13. D'Agostino RB Sr., Vasan RS, Pencina MJ, et al. General cardiovascular risk profile for use in primary care: the Framingham Heart Study. *Circulation*. 2008;117(6):743–753.
14. Chao M, Schreibmann E, Li T, Koong A, Goodman KA, Xing L. Automatic contouring in 4D radiation therapy. *Int J Radiat Oncol*. 2006;66(3):S649.
15. Han X, Hoogeman MS, Levendag PC, et al. Atlas-based auto-segmentation of head and neck CT images. *Med Image Comput Comput Assist Interv*. 2008;11(pt 2):434–441.
16. Wang H, Garden AS, Zhang L, et al. Performance evaluation of automatic anatomy segmentation algorithm on repeat or four-dimensional computed tomography images using deformable image registration method. *Int J Radiat Oncol Biol Phys*. 2008;72(1):210–219 doi:S0360-3016(08)00802-X [pii] 10.1016/j.ijrobp.2008.05.008.
17. Reed VK, Woodward WA, Zhang L, et al. Automatic segmentation of whole breast using atlas approach and deformable image registration. *Int J Radiat Oncol Biol Phys*. 2009;73(5):1493–1500. doi: S0360-3016(08)02980-5 [pii] 10.1016/j.ijrobp.2008.07.001.
18. Eldesoky AR, Yates ES, Nyeng TB, et al. Internal and external validation of an ESTRO delineation guideline-dependent automated segmentation tool for loco-regional radiation therapy of early breast cancer. *Radiother Oncol*. 2016;121(3):424–430. doi:0.1016/j.radonc.2016.09.005.
19. Chao KS, Bhide S, Chen H, et al. Reduce in variation and improve efficiency of target volume delineation by a computer-assisted system using a deformable image registration approach. *Int J Radiat Oncol Biol Phys*. 2007;68(5):1512–1521 doi:S0360-3016(07)00693-1 [pii] 10.1016/j.ijrobp.2007.04.037.
20. Stapleford LJ, Lawson JD, Perkins C, et al. Evaluation of automatic atlas-based lymph node segmentation for head-and-neck cancer. *Int J Radiat Oncol Biol Phys*. 2010;77(3):959–966. doi:10.1016/j.ijrobp.2009.09.023.
21. Dormer JD, Halicek M, Ma L, Reilly CM, Schreibmann E, Fei B. Convolutional neural networks for the detection of diseased hearts using CT images and left atrium patches. *Proc SPIE Int Soc Opt Eng*. 2018;10575:1057530. doi:10.1117/12.2293548.
22. Dormer JD, Ma L, Halicek M, Reilly CM, Schreibmann E, Fei B. Heart chamber segmentation from CT using convolutional neural networks. *Proc SPIE Int Soc Opt Eng*. 2018;10578:105782S. doi:10.1117/12.2293554.
23. Aerts HJ, Velazquez ER, Leijenaar RT, et al. Decoding tumour phenotype by noninvasive imaging using a quantitative radiomics approach. *Nat Commun*. 2014;5:4006. doi:10.1038/ncomms5006.
24. Bureau International des Poids et Mesures (BIPM). The International System of Units (SI), Secondary. 2010. https://www.bipm.org/en/home.
25. Foley J, van Dam A, Hughes J, Feiner S. *Computer Graphics: Principles and Practice*. WIllard, OH: Addison-Wesley; 1990.